Proceedings of the XVIII ECSMGE 2024
GEOTECHNICAL ENGINEERING CHALLENGES
TO MEET CURRENT AND EMERGING NEEDS OF SOCIETY

ISBN 978-1-032-54816-6
DOI 10.1201/9781003431749-687

ECSMGE 24
XVIII EUROPEAN CONFERENCE ON SOIL MECHANICS AND GEOTECHNICAL ENGINEERING

Reinforcement of a coarse granular aggregate with microgrids: Influence on packing

Renforcement d'un agrégat granulaire grossier à l'aide de micro-grilles: Influence sur le paquetage

R. Anjos*, M. Pinho-Lopes
RISCO, Department of Civil Engineering, University of Aveiro, Aveiro, Portugal
W. Powrie
School of Engineering, University of Southampton, Southampton, United Kingdom
**rafaelanjos@ua.pt*

ABSTRACT: Micro-reinforcement using engineered fibres or particulate inclusions, such as strip fibres, has potential for improving the performance of coarse granular aggregates, such as materials for road bases or railway ballast. During loading, the aggregate particles move, and the soil skeleton is rearranged. Recent studies have shown the effectiveness of fibre reinforcement of soils and coarse granular aggregates. Usually, the fibres are mixed randomly within the soil skeleton, with consequences on packing. Fibres can be considered micro-reinforcements, as these are inclusions at the particle scale. Alternatively, other forms of micro-reinforcements can be used. Small elements of geogrids, herein designated microgrids, are alternative forms of micro-reinforcement. Their inclusion may also affect the packing of the particles of aggregate, as the presence of the reinforcement my affect the displacement and rotation of the adjacent particles. In this paper, the influence of microgrids on the packing of a coarse aggregate is analysed. For that, a container with two transparent faces was used. The aggregate and the micro-reinforcement elements were mixed at a predetermined volumetric ratio, placed in the container, and submitted to compaction. The addition of microgrids disrupted the natural grain packing, and corresponding increases in e_{max} and e_{min} were observed. For the microgrid with higher anchorage length, non-natural void formation was observed due to microgrid-microgrid interaction rather than microgrid-grain interlocking.

RÉSUMÉ: Le micro-renforcement à l'aide de fibres artificielles ou d'inclusions particulaires, telles que les fibres en bandes, peut améliorer les performances des agrégats granulaires grossiers, tels que les matériaux pour les bases routières ou le ballast des voies ferrées. Pendant le chargement, les particules d'agrégats se déplacent et le squelette du sol est réorganisé. Des études récentes ont montré l'efficacité du renforcement des sols et des agrégats granulaires grossiers par des fibres. En général, les fibres sont mélangées de manière aléatoire dans le squelette du sol, ce qui a des conséquences sur le paquetage. Les fibres peuvent être considérées comme des micro-renforts, car il s'agit d'inclusions à l'échelle des particules. D'autres formes de micro-renforts peuvent également être utilisées. Les petits éléments des géogrilles, appelés ici micro-grilles, sont d'autres formes de micro-renforcement. Leur inclusion peut également affecter le paquetage des particules de l'agrégat, car la présence du renforcement peut affecter le déplacement et la rotation des particules adjacentes. Dans cet article, l'influence des micro-grilles sur le paquetage d'un agrégat grossier est analysée. Pour ce faire, un conteneur à deux faces transparentes a été utilisé. L'agrégat et les micro-éléments de renforcement ont été mélangés selon un rapport volumétrique prédéterminé, placés dans le conteneur et soumis au compactage. L'ajout de micro-grilles a perturbé l'empilement naturel des grains, et des augmentations correspondantes d'e_{max} et d'e_{min} ont été observées. Pour la micro-grille ayant une longueur d'ancrage plus élevée, on a observé une formation de vides non naturels due à l'interaction micro-grille-micro-grille plutôt qu'à l'imbrication micro-grille-grain.

Keywords: Micro-reinforcement; packing; coarse aggregates; scaled-ballast.

1 INTRODUCTION

For the past two decades, researchers (Lirer et al. 2011; Michalowski & Čermák, 2003; Soriano et al. 2017) have tried to reinforce soils, mostly sands, with random micro-reinforcements, such as discrete fibres. The shear strength of the resulting composite material is governed by the micro and the macromechanical characteristics of both fibres and soil particles (Lirer et al. 2011). Discrete fibres play a significant role in increasing the overall shear strength and ductility of sands (Michalowski & Čermák, 2003). Because of the effectiveness of fibre reinforcement, the approach has been extended to coarse granular aggregates such as railway ballast.

Railway ballast is a coarse granular aggregate, generally obtained by quarrying high quality rock, used as a load bearing layer. The ballast layer supports the track superstructure and transfers the load generated at wheel-rail interface to the sub-base and the underlying soil. Laboratory testing of full-size ballast is difficult, expensive, and time-consuming. Thus, testing scaled-down ballast is an attractive solution for understanding the mechanics of full-size ballast (Sevi, 2008).

Ajayi et al. (2017a) studied the behaviour of 1/3 and 1/5 scaled ballast reinforced with randomly distributed strip fibres and analysed the influence of the fibre dimensions and fibre content. Ajayi et al. (2017a) observed that, in monotonic triaxial tests, fibre-reinforced gravels exhibited decreased dilation, increased ductility and increased peak deviator stress. Within the framework of classic soil mechanics principles, reduced dilatancy is consistent with higher ductility, but neither is consistent with an increased deviator stress. Thus Ajayi et al. (2017a) proposed a three-phase model for the grains, fibres and voids, with the fibres considered explicitly as a separate phase:

$$\upsilon = \frac{V_s+V_f+V_v}{V_s} = 1 + e + V_{fr} \qquad (1)$$

where υ is the specific volume of fibre-reinforced soil, V_s is the volume of solids, V_f is the volume of fibres, V_v is the volume of voids, e is the void ratio of the soil (considering soil particles only) and V_{fr} is the volumetric fibre ratio (V_f/V_s). This framework has the advantage of considering the fibres independently of the natural soil matrix (solids particles and voids).

Ajayi et al. (2017a) expressed the fibre dimensions normalised with respect to the effective diameter corresponding to 50% of soil particles, D50. LN is the normalised fibre length (= Lf/D50) and WN the normalised fibre width (= Wf/D50), where Lf is the fibre length and Wf is the fibre width.

For the case of 1/3 scale ballast reinforced with strip fibres, the minimum normalised fibre dimensions giving an effective improvement of the monotonic response were: LN = 7.1 and WN = 2.5 (Ajayi et al. 2017a). The volumetric fibre ratio, Vfr, is the ratio in Eq.1 that accounts for the presence of fibres in the soil matrix. For a given Vfr, as the grain size increases, the number of fibres required to develop similar grains–fibre interactions decreases. Thus for scaling purposes, Vfr is not a sufficient measure for representing the fibre content. When considering the mechanical behaviour of fibre reinforced granular materials across different grain size ranges, the number of fibres available for fibre-grain interaction is also important and can be defined by the fibre-grain ratio Nfg. For a given fibre length and width, Nfg is the ratio between Nf, the number of individual fibres in a fibre reinforced specimen and Ng the number of grains in a fibre reinforced specimen. Ng can be estimated using two different approaches: Approach 1, which assumes that all grains are approximately spherical with a diameter equal to D50 (Ajayi et al. 2017b); Approach 2, which divides the weight of the ballast specimen by the average weight of a single grain (Ferro et al. 2023).

Ferro et al. (2022) studied the ability of randomly distributed fibres to reinforce full-size ballast using packing tests and full-scale cyclic laboratory tests (single sleeper bay section of railway under plane strain conditions). From the full-scale tests, the authors concluded that the effectiveness of fibres in reducing the settlement of traditional railway track depends not only on their ability to increase the material shear resistance, but also on how little they influence the packing of ballast grains. To assess the effect of fibre reinforcement on the long-term settlement of ballast after cyclic load, Ferro et al. (2022) proposed an alternative measure of the propensity to pack of the fibre-reinforced composite, IDr:u which is the ratio of the range of reinforced void ratios (emax and emin, maximum and minimum void ratio of unreinforced ballast) to the corresponding range the unreinforced material (e^U_{max} and e^U_{min}, maximum and minimum void ratio of unreinforced ballast, respectively). For full-size ballast IDr:u should be smaller than 1.05 (Ferro et al. 2022).

The form of the reinforcement will result in different mobilisation mechanisms. Discrete fibres oriented horizontally can sustain tensile forces generated at the grains level (Soriano et al. 2017), while microgrids will tend to generate additional interaction mechanisms such as local interlocking. Indraratna et al. (2018) analysed geogrid reinforcement of railway ballast and defined a range for the geogrid aperture size, A, that maximise bearing capacity of the ballast layer, while reducing track settlement. The aperture size should not be smaller than 0.9D50 and larger than 1.2D50.

In this paper, two forms of microgrid were studied, particularly their effect on the packing of a coarse granular aggregate. Unreinforced and reinforced specimens were compacted using a shaking table and the effect of compaction on the grain packing was analysed.

2 MATERIALS AND METHODS

2.1 Materials

Freshly quarried gneiss granular aggregate was obtained from *Irmãos Cavaco* quarry (Aveiro, Portugal). This coarse material corresponds to a 1/3 scale representation of the full-size ballast used on Portuguese railways (BS EN 13450: Aggregates for Railway Ballast, 2013). The particle size distribution of the aggregate is shown in Figure 1. G_s is the aggregate specific gravity, C_u is the uniformity coefficient and *FI* the flakiness index. *FI* informs about the percentage by weight of an aggregate with an aspect ratio less than 0.6 times their mean size. The natural effective angle of shearing resistance (effective angle of friction), ϕ', of the coarse granular aggregate is 39°.

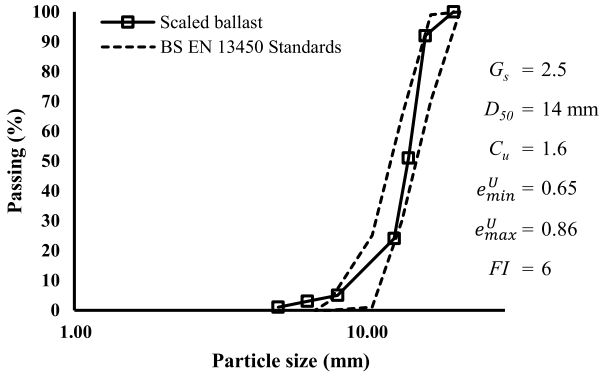

Figure 1. Aggregate particle size distribution and additional properties.

The microgrids were obtained from a commercially available geogrid by cutting pieces to a predefined geometry. Two different microgrid shapes were considered (Figure 2). The normalised dimensions of the microgrids are given in Table 1.

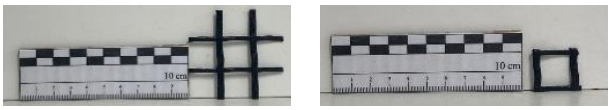

a) *b)*

Figure 2. Microgrids studied: a) MG1, b) MG2.

Table 1. Microgrids volume and normalised geometry: length, width, and aperture size.

Normalised dimensions	MG1	MG2
Volume of a single element (cm^3)	0.554	0.238
L_N (-)	3.9	1.8
W_N (-)	3.7	1.6
A/D_{50} (-)	1.1	1.1

The central element of MG1 and MG2 is the same (an opening of 16 mm × 16 mm). The difference between MG1 and MG2 is that the former includes additional elements beyond the central element (Figure 2). Thus, the normalised length and width of MG1 are nearly double of MG2. The normalised aperture size (A/D_{50}) of the microgrids is within the range proposed by Indraratna et al. (2018). However, the normalised length (L_N) and width (W_N) of the microgrids do not meet the optimum dimensions proposed by Ajayi et al. (2017a), for strip fibres.

2.2 Packing test

To assess the effect of the microgrids on the packing of the 1/3 scale ballast grains, packing tests were carried out. Two different plywood boxes were used: Box 1, cubic box with internal edges of 300 mm (all faces made 16 mm thick plywood); Box 2, cubic box with two 8 mm thick plexiglass faces, which allow for visual inspection of the particle movement during compaction, with longitudinal internal edges (268 and 300 mm). The boxes were stiff enough to ensure plane strain conditions. The packing tests were carried out in Box 1, and visual observation of the packing using Box 2.

For each packing test, Box 1 was filled manually and weighed. Loose conditions were obtained by placing the aggregate gently into the box. Dense conditions were obtained using a shaking table, with a frequency of 50 Hz and amplitude of 0.8 mm. Three episodes of shaking (approximately 300 seconds each) were applied after placing each layer of material (100 mm high) into the box, with a total of 3 layers. The box was slightly overfilled and the final top surface levelled by adding and removing individual grains. For the dense condition, the final level was obtained by hand-pressing the lid against the aggregates while vibrating. This process, described by Ferro et al. (2022), allows the maximum density to be achieved without grain breakage. Once the specimen had been levelled, the lid was placed on top of it and the actual height of aggregate was measured.

The packing tests (Box 1) were carried out for a predetermined volumetric fibre ratio of 3.2%, identified by Ajayi et al. (2017a) as the optimum Vfr for a coarse granular aggregate with grain dimensions similar to that used herein. The volume of microgrid reinforcement was calculated from the volume of solid particles and the bulk density of the specimen. Mineral particles were hand-mixed with microgrids on a specimen by specimen basis to ensure a random distribution of the microgrids within the grains.

For each condition (unreinforced, U; reinforced with microgrid 1, R MG1, and with microgrid 2, R MG2), 6 packing tests were carried out; 3 for the loosest (emax) and 3 for the densest (emin) condition,

resulting in a total of 18 tests. One additional packing test per condition was carried out in Box 2 (3 tests in total).

3 RESULTS AND DISCUSSION

3.1 Fibre-grain ratio

To assess the fibre-grain ratio, N_{fg}, it is necessary to estimate the number of grains per specimen. Table 2 summarises the estimates of the number of grains average value for 3 specimens per condition tested, N_g, using Approaches 1 (Ajayi et al. 2017b) and 2 (Ferro et al. 2023), described in section 1.

Table 2. Number of grains, N_g, and fibre-grain ratio, N_{fg}, for the specimens tested, using Approaches 1 (Ajayi et al. 2017b) and 2 (Ferro et al. 2023).

Nomenclature	U	R MG1	R MG2
V_{fr} (%)	-	3.2	3.2
N_g (-) Ajayi et al. (2017b)	11675	9914	10422
N_g (-) Ferro et al. (2023)	12175	10339	10867
N_{fg} (%) Ajayi et al. (2017b)	-	9.8	21.7
N_{fg} (%) Ferro et al. (2023)	-	9.4	20.8

Approach 2, proposed by Ferro et al. (2023), leads to higher number of grains per specimen (by ~4%) than the method proposed by Ajayi et al. (2017b). The different estimates of N_g influence the fibre-grain ratio, which are related to the volume of a single fibre. To better understand those relations, Figure 3 shows the influence of the volume of a single fibre on the fibre-grain ratio, N_{fg}. (for a constant volume of solids, V_s = 0.017 m^3, and volumetric fibre ratio, V_{fr}). As the volume of a single fibre increases, the number of grains that potentially can be engaged by each fibre decreases. The average volume of a single fibre MG1 and MG2 is, respectively 0.554 cm^3 and 0.238 cm^3. The differences in N_{fg} between the two approaches are small (Table 2, Figure 3). This is related to the shape of the aggregate particles studied: a reduce flakiness index, $FI \leq 15\%$, indicates that most grains have a reasonably spherical shape. For materials with higher FI, the approach proposed by Ferro et al. (2023) will tend to be more realistic.

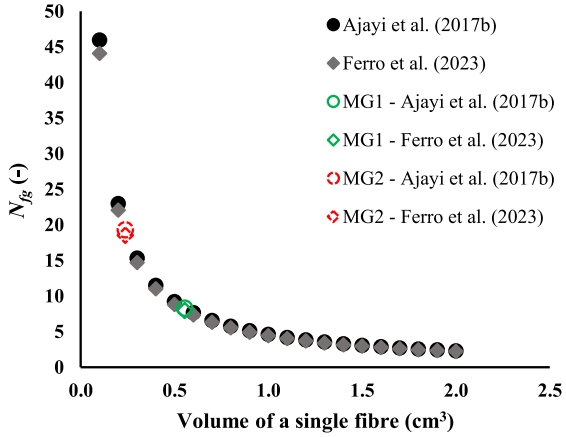

Figure 3. Variation of the fibre-grain ratio with the volume of a single fibre.

3.2 Packing

Table 3 summarises the packing test results (average for three specimens per condition); the maximum and minimum void ratio (e_{max} and e_{min}) and the ratio of the range of reinforced void ratios to that of the unreinforced material ($I_{Dr:u}$).

Table 3. Packing test results (average for 3 specimens per condition), maximum (e_{max}) and minimum (e_{min}) void ratio, standard deviation (σ), and grains packing disruption analysis ($I_{Dr:u}$).

Nomenclature	e_{max} (-)	σ (-)	e_{min} (-)	σ (-)	$I_{Dr:u}$ (-)
U	0.86	0.01	0.65	0.01	-
R MG1	1.42	0.02	0.93	0.02	2.25
R MG2	1.12	0.01	0.86	0.01	1.20

The addition of microgrids at V_{fr} = 3.2% led to an increase in both the maximum and the minimum void ratio of the mix relative to the unreinforced aggregate. For MG1, e_{max} increased by 64% and e_{min} by 33%; for MG2, this effect was less pronounced, with increases of 29% for e_{max} and 24% for e_{min}. Both microgrids interfered significantly with the natural packing of the aggregate grains, as $I_{Dr:u} > 1.05$. MG1, owing to its form and greater length than MG2, caused greater disruption to the natural packing with $I_{Dr:u}$ = 2.25.

The packing tests carried out in Box 2 allowed observation of the relative positions of the microgrids and grains, and changes during loading. Figure 4 shows cross sections of specimens, unreinforced and reinforced with MG1 and MG2, at different stages of the test: initial state, t = 0 s; half way through compaction, t = 150 s; and after compaction, t = 300 s. The distribution and arrangement of the microgrids on horizontal cross sections was also observed on

disassembling the boxes following the end of each test (plan view, Figure 4g and k).

The inclusion of microgrids MG1 and MG2 influenced the packing of the aggregate (Figure 3a, d and h). Particularly for MG1, the number and dimension of the voids in the vicinity of MG1 is important. Although the specimen R MG1 (as indicated by the values of emax and emin, Table 3) densified during compaction, the process did not eliminate such voids. Thus MG1 clearly disrupted the natural packing of the aggregate. For MG2, this was less evident, indicating that the form of MG2 is more easily accommodated by the aggregate particles than that of MG1.

Microgrid segregation was observed in both cases, and was more pronounced for MG1 than MG2. Again, this can be explained by the different forms of the microgrid reinforcements.

The results (Table 3) and the observations of the disrupted packing (Figure 4, with fibre overlapping) indicate that V_{fr} = 3.2 % is not optimum for this type of micro-reinforcement. However, this value was proposed by Ajayi et al. (2017a) for strip fibres not for microgrids. Thus further studies to optimise the form and the corresponding content of microgrids are needed.

During filling of Box 2 and at the start of the packing tests, it was evident that some microgrids were vertically oriented along the plexiglass. For this reason, at the end of the test the box was emptied carefully, in layers, to check if this was a boundary effect. The microgrid elements were found at both horizontal and vertical positions in all plan sections of the specimens (Figure 4). This is likely a consequence of the stabilisation effect that microgrids have, as they tend to lock-in aggregate particles in their vicinity and rotate along with grains.

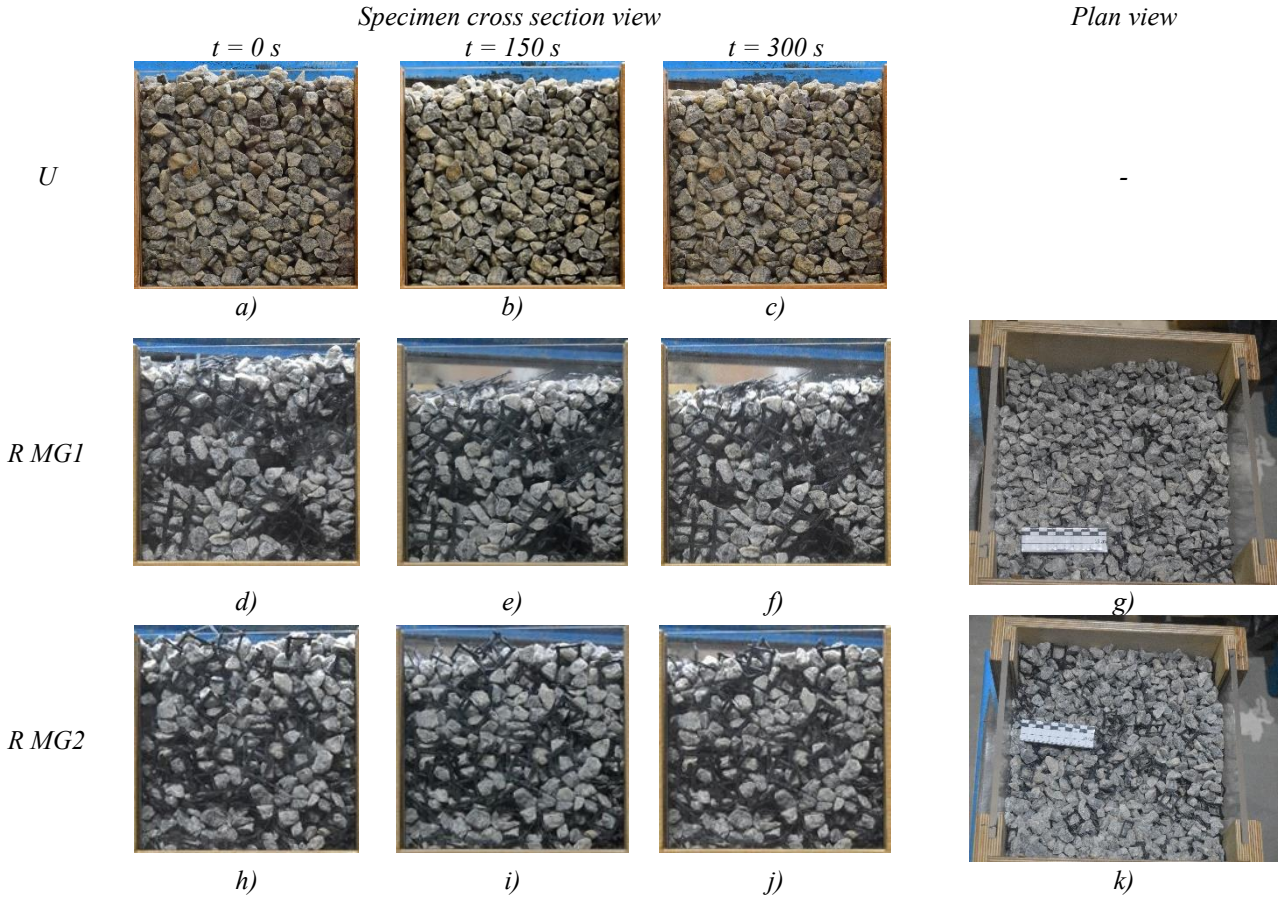

Figure 4. Cross section view of the packing tests (Box 2) at different moments: initial state (t = 0 s) a) U, d) MG1, h) MG2; after half way through compaction (t = 150 s) b) U, e) MG1, i) MG2; after compaction (t = 300 s) h) U, i) MG1, j) MG2, Plan view of specimens after compaction (Box 2) showing microgrid orientation: g) MG1, k) MG2.

4 CONCLUSIONS

In this paper, the reinforcement of a coarse aggregate (1/3 scale railway ballast) with two different types of microgrid was investigated using packing tests. The fibre-grain ratio was estimated using two different approaches from the literature. Images taken during the packing tests were analysed, to better understand

how the microgrids influence packing of aggregate particles. The main conclusions from the study are:

1. The inclusion of the microgrids influenced the aggregate packing and increased the maximum and minimum void ratios of the mix relative to the unreinforced aggregate.
2. The form of the microgrids affected the degree of disruption; the smaller microgrid, with only a central square element, was less disruptive.
3. The approaches used to estimate the number of grains per specimen gave similar results (4% difference).
4. The optimum volumetric fibre ratio V_{fr}= 3.2% for strip fibre reinforcement of similar aggregates is not appropriate for the microgrid reinforcements studied.
5. In contrast to strip fibre reinforcement, which adopt a generally horizontal orientation, microgrids orientate both vertically and horizontally within the aggregate particles.

Additional studies are needed to determine the optimum volumetric fibre ratio for microgrids and to give a better understanding of the micro mechanical interaction between microgrids and grains. Optimisation of the form of micro-reinforcement seems possible and needs further investigation.

ACKNOWLEDGEMENTS

The financial support of FCT ("Fundação para a Ciência e Tecnologia" – Portugal) is gratefully acknowledged through the project UIDB/04450/2020 (RISCO).

This research was supported by the doctoral Grant PRT / BD / 154385 / 2022 financed by Portuguese Foundation for Science and Technology (FCT), and with funds from The State Budget, from the European Social Fund (ESF) made available under Reginal Operational Program of the Center (Centro 2020), under MIT Portugal Program.

REFERENCES

Ajayi, O., Le Pen, L., Zervos, A., & Powrie, W. (2017a). A behavioural framework for fibre-reinforced gravel. *Géotechnique*, *67*(1), 56–68. https://doi.org/10.1680/JGEOT.16.P.023.

Ajayi, O., Le Pen, L., Zervos, A., & Powrie, W. (2017b). Scaling relationships for strip fibre reinforced aggregates. *Canadian Geotechnical Journal*, *54*. https://doi.org/10.1139/cgj-2016-0346.

BS EN 13450: (2013) Aggregates for railway ballast, Pub. L. No. 13450, BSI Standards Publication.

Ferro, E., Le Pen, L., Zervos, A., & Powrie, W. (2022). Fibre-reinforcement of railway ballast to reduce track settlement. *Géotechnique*, *0*(0),1-13 https://doi.org/10.1680/jgeot.21.00421.

Ferro, E., Le Pen, L., Zervos, A., & Powrie, W. (2023). Reducing the settlement of railway ballast by random fibre reinforcement. In *Geosynthetics: Leading the Way to a Resilient Planet* (pp. 1366–1371). CRC Press. https://doi.org/10.1201/9781003386889-175.

Indraratna, B., Ferreira, F. B., Qi, Y., & Ngo, T. N. (2018). Application of geoinclusions for sustainable rail infrastructure under increased axle loads and higher speeds. *Innovative Infrastructure Solutions*, *3*(1). https://doi.org/10.1007/s41062-018-0174-z.

Lirer, S., Flora, A., & Consoli, N. C. (2011). On the strength of fibre-reinforced soils. *Soils and Foundations*, *51*(4), 601–609. https://doi.org/10.3208/sandf.51.601.

Michalowski, R. L., & Čermák, J. (2003). Triaxial Compression of Sand Reinforced with Fibers. *Journal of Geotechnical and Geoenvironmental Engineering*, *129*(2), 125–136. https://doi.org/10.1061/(asce)1090-0241(2003)129:2(125).

Sevi, A. F. (2008). *Physical modeling of railroad ballast using the parallel gradation scaling technique within the cyclical triaxial framework*. University of Missouri.

Soriano, I., Ibraim, E., Andò, E., Diambra, A., Laurencin, T., Moro, P., & Viggiani, G. (2017). 3D fibre architecture of fibre-reinforced sand. *Granular Matter*, *19*(4). https://doi.org/10.1007/s10035-017-0760-3.